Chalcogenide Letters Vol. 19, No. 9, September 2022, p. 579 - 590

Synthesis and characterization of Cu_2S:Al thin films for solar cell applications

A. A. Hamid[a,*], B. K. H. Al-Maiyaly[b,*]
Department of physics, College of Education For Pure Science (Ibn Al-Haitham), University of Baghdad, Baghdad, Iraq

In this work Nano crystalline (Cu_2S) thin films pure and doped 3% Al with a thickness of 400±20 nm was precipitated by thermic steaming technicality on glass substrate beneath a vacuum of $\sim 2 \times 10^{-6}$ mbar at R.T to survey the influence of doping and annealing after doping at 573 K for one hour on its structural, electrical and visual properties. Structural properties of these movies are attainment using X-ray variation (XRD) which showed Cu_2S phase with polycrystalline in nature and forming hexagonal temple ,with the distinguish trend along the (220) grade, varying crystallites size from (42.1-62.06) nm after doping and annealing. AFM investigations of these films show that increase average grain size from 105.05 nm to 146.54 nm while decrease the roughness from 5.93 nm to 4.73 nm after doping. Hall measurements show that the conductivity change from 1.43×10^{-3} to 7.33×10^{3} $(\Omega\,cm)^{-1}$, these films have p-type conductivity and the mobility varied from 3.87×10^{2} to 8.48×10^{10} $cm^2/V.s$. Optical constants were calculated for these films in the range of wave length (300-1100) nm using UV/Visible measurement. The visual properties showed that Cu_2S membrane have a high value of the absorption coefficient and decrease the optical energy gap values from (2.25-1.5) eV after doping with 3% Al. The characterization of these films can chose in the application of solar cells.

(Received May 16, 2022; Accepted September 2, 2022)

Keywords: Cu_2S, Doping, Thermal evaporation, Thin films

1. Introduction

Thin films Copper sulphide are considered especially as p-type semiconductors as promising materials for solar energy conversion systems, due to their structural, optical and electrical properties [1 B]. In recent years the investigations of Cu_2S thin films has recipient enormous notice because of to their potential in a photovoltaic cell and it's abundant technological implementations in the accomplishment of solar cell, tubular solar cells, in photovoltaic diversions of solar energy [2-9], automobile glazing, as solar absorber coating, dye-sensitized solar cells, photo detector, microwave shielding coatings and as sensors etc. [10-13].

Thin films copper sulphide have been deposition by diverse preparation methods like reactive magnetron sputtering [14], alchemical bathroom precipitation [1,15-18], drizzle pyrolysis [19], consecutive ionic stratum adsorption and reaction [20], microwave assisted chemical bath precipitation [21] , thermal steaming [9] and chemical vapor deposition [22]. In the present paper, thin films copper sulfide were prepared by thermic vaporization and the impact of 3% Al doping and then annealing at 573 K on structural and visual properties was attainment.

* Corresponding authors: boshra.k.h@ihcoedu.uobaghdad.edu.iq
https://doi.org/10.15251/CL.2022.199.579

2. Experimental Details

(Cu_2S) alloy was prepared throughout mixing high purity (99.99%) copper (Cu) and sulfur (S) elements in a ratio of (1:1) according to the proper atomic weight, then placed in evacuated quartz tube, which heated at 1273 K in a thermal furnace for five hours, later left to cool to R.T. The tube was taken out from the furnace, and was broken from one end to extract the composite ingot from it, which was ground by a special mill (laboratory mill) to obtain the powder of the material. Cu_2S thin films were prepared from powder on glass substrates at R.T of 400 nm thicknesses by thermal evaporation technique under vacuum of ~10^{-5} mbar, then doping these films with 3% Al and then subjected to heat treatment at 573 K for one hour. The structures of Cu_2S alloy and all films pure and doped have been studied by X–ray diffraction technique using (SHIMADZU-Japan-XRD 6000) diffract meter system with CuKα radiation· (λ = 1.5418 Å), 20 mA current and 40Kv voltage, as well as the optical and Hall measurement have been done.

3. Results and discussions

3.1. X-ray Diffraction Analyses

Figure (1) show the XRD spectrum of Cu_2S thin films pure and doped 3% Al at (R.T and Ta=573 K) deposited by thermal evaporation technique with (400nm) thickness. All these XRD pattern show polycrystalline nature of films and formation of Cu_2S phase which is indexed in the standard ICDD (00-053-0522) card where peaks at 2θ= 16.027, 36.33, 45.99, 51.82 and 54.40 corresponding to (100), (210), (210), (220), (310), (311) respectively. As well as XRD patterns show that all films prepared have single phase crystal and highly pure due to no secondary phase is detected. In addition, the preferred orientation along (220) plane increased, peaks get sharper and crystalline size improvement after doping and annealing (at Ta=573 K) which means grown of Nano crystallite size.

Using Scherer's equation, the size of the crystals is estimated.. [23]:

$$C.S=\frac{0.94\lambda}{\beta COS\theta} \quad (1)$$

where λ: represents the XRD wave length, β: represents the FWHM of the peaks, and θ: represents Bragg's angle. Williamson and Smallman's equation was used to compute the dislocation density (δ). [23]. Tables 1 and 2 contain all of these values for Cu_2S alloy and films respectively.

$$\delta = \frac{1}{(C.S)2} \quad (2)$$

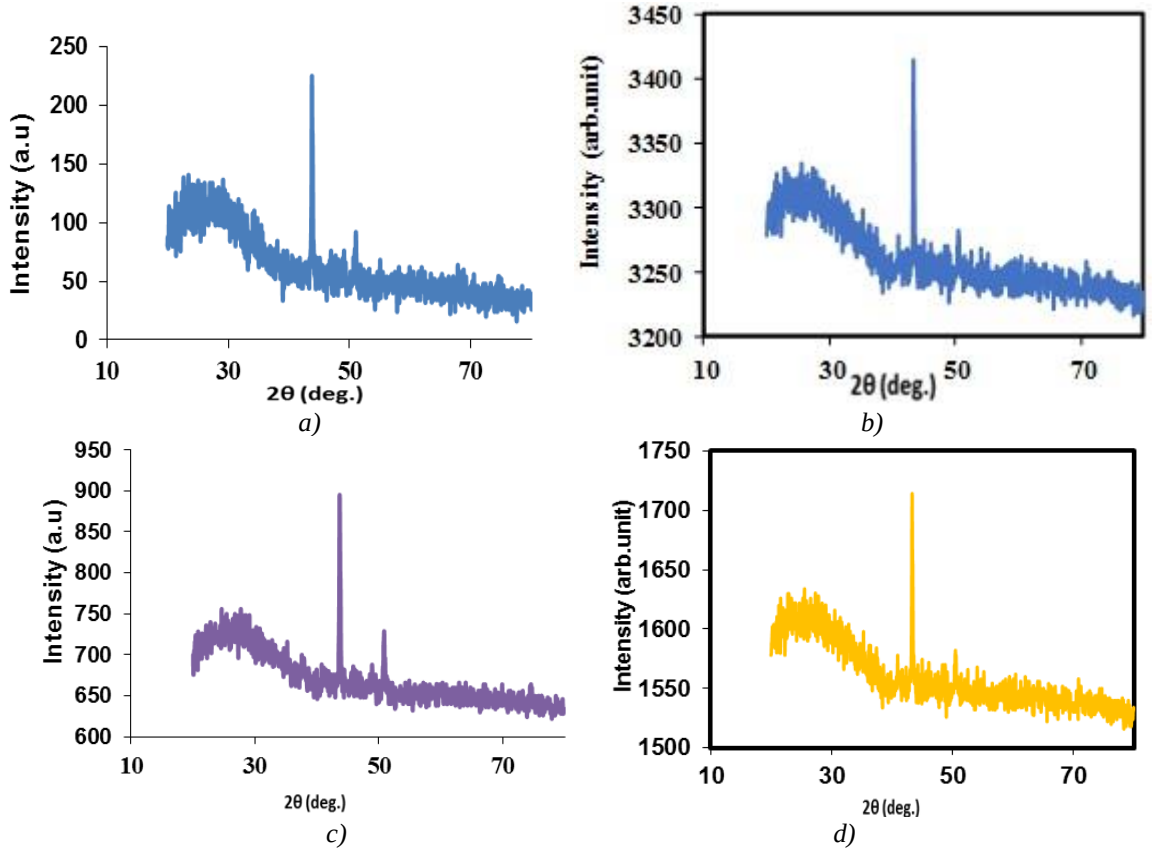

Fig. 1. XRD of Cu_2S thin films of:
a) pure at R.T b) pure at Ta=573 K c) doped 3% Al at (273k) d) doped 3% Al at (Ta=573 K).

Table 1. Structural parameters for Cu_2S alloy.

2θ (Std.) (Deg.)	2θ (Exp.) (Deg.)	d(Std) (Å)	d(Exp) (Å)	hkl	FWHM (Deg.)	C.S (nm)	a(Std.) (Å)	a(Exp.) (Å)
15.9152	16.0272	5.564000	5.52550	100				
36.1076	36.3375	2.485500	2.47036	210				
46.1034	45.9980	1.967200	1.97151	220	0.39570	22.7998	5.564Å	5.570Å
51.9251	51.8274	1.759500	1.76263	310				
54.6724	54.4014	1.677400	1.68516	311				

Table 2. Structural parameters for Cu_2S.

Sample	T(°C)	2θ	FWHM(deg)	d_{hkl} (exp) A°	$d_{hkl\ (std)}$ A°	C.S (nm)	$\delta * 10^{15}$ (lines/m^2)
Cu_2S	R.T	43.8375 51.0178	0.21220 0.30000	2.0723 1.7900	2.0635 1.7886	42.1583 30.659	0.000562 0.00107
Cu_2S	300	35.5424 38.7098	0.5900 0.7000	2.5257 2.3260	2.5237 2.3242	14.7747 12.5697	0.00458 0.006329
Cu_2S (Al)	300	36.3576 42.3073	0.3352 0.2500	2.4709 2.1362	2.4690 2.1345	62.0654 35.6032	0.00147 0.000788

3.2. AFM Measurement

AFM were used to examined surface morphology of Cu_2S films pure and doped 3% Al at (R.T and Ta=573 K). Figure (2) show three dimensional (3D) AFM images of Cu_2S films, these images show that all films uniform fashion without any cracks or pinholes and packed together distributed of Nano sized grains. Table (3) show AFM results, it can be deduced from this table that average grain size increase from (105.05)nm to (146.54)nm, the toughness of film surfaces increases, root-mean square RMS surface changed after doping and annealing (at Ta=573 K) due to structure improvement which agreement with X- ray diffraction results. Low roughness and uniform characterizing, can play good role for properties of photovoltaic cell.

Table 3. AFM results for Cu_2S thin films.

Thin Films	T_a (K)	Surfaces roughness (nm)	Root mean Sq. (nm)	Grain Size (nm)
Pure	RT 300	5.93 23.8	7.16 29.5	105.05 170.82
Cu_2S (Al)	RT 300	4.73 5.28	5.92 6.91	146.54 141.19

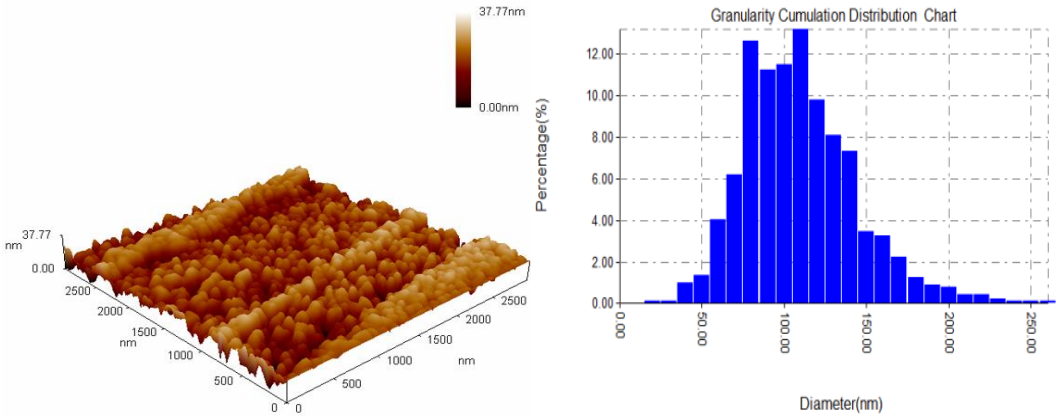

(a)

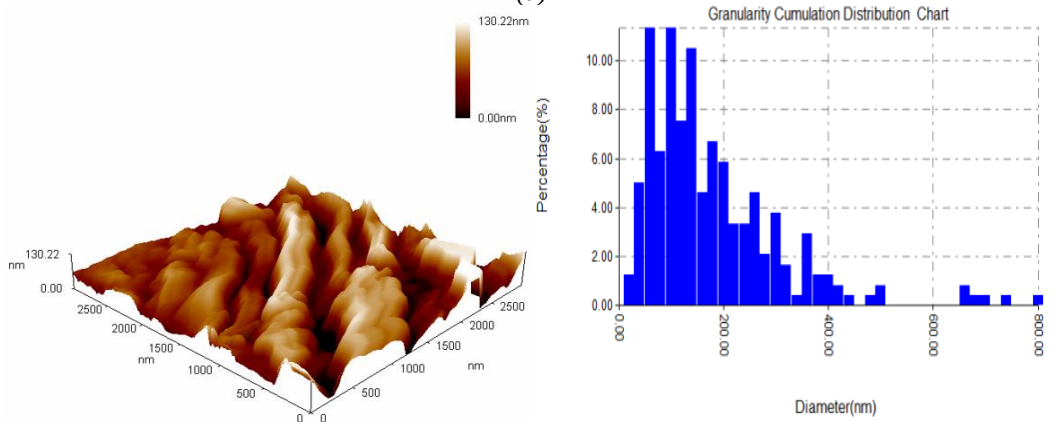

(b)

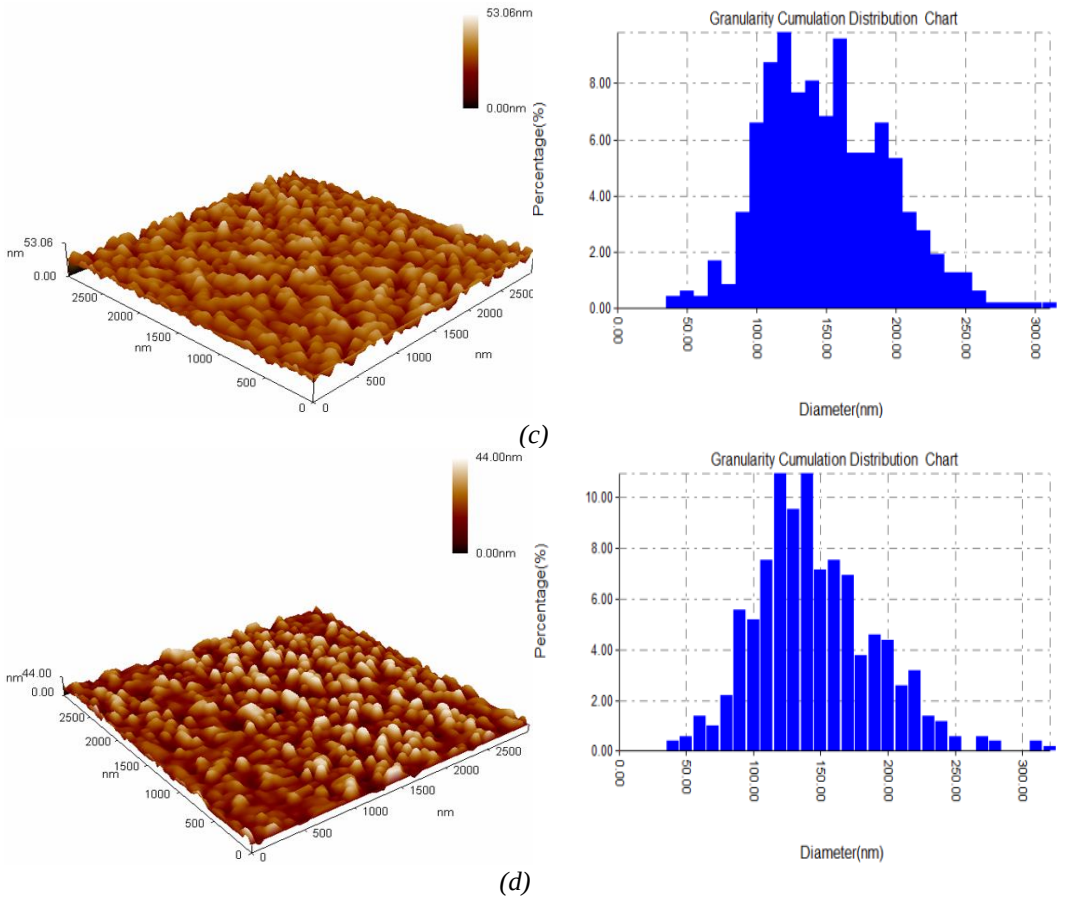

Fig. 2. AFM images of Cu_2S thin films a) pure at R.T b) pure at Ta=573 K c) doped 3% Al at (273k) d) doped 3% Al at (Ta=573 K).

3.3. Optical Measurement

The absorbance (A) as a function of wavelength extent (300 – 1000) nm for Cu_2S thin films pure and doped 3% Al at (R.T and Ta=573 K) are shown in figure (3) . This shape indicates the absorption values increment after doping and annealing due to lowering cereal border and development tiny cereal while decreased with increase wave length. Also high absorption value appear at extent of wavelength (400-600) nm, making Cu_2S movies relevance for solar cell implementations.

Figure (4) shows the permeability (T) of Cu_2S thin films pure and doped 3% Al at (R.T and Ta=573 K). It is clear from this shape that the value of the permeability increases with an increase wave length and the high values in the NIR area while decrease after doping and annealing, this behavior regarding to the variations in crystal structure after doping and annealing.

All Cu2S films have significant absorption coefficients ($\alpha > 10^4$ cm^{-1}) as shown in form (5). This indicates that a permissible direct transition is likely. As well as from this shape, it can be seen that the values of the absorption coefficient increase after doping and annealing and displacement to lower energy because The absorption is not only the responsibility of the freedom bearersbut to impurities or electronic states in a stationary state.

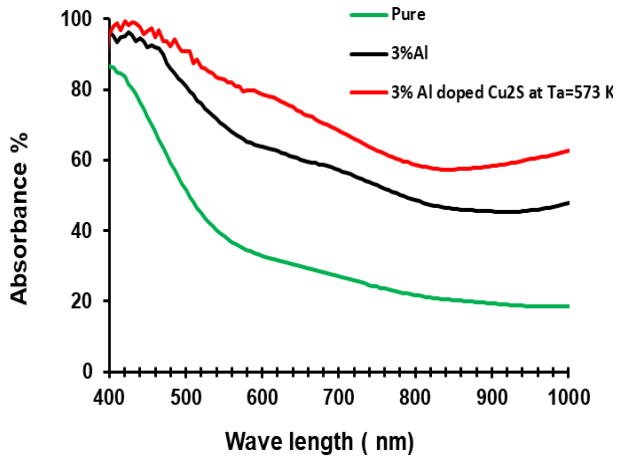

Fig. 3. Absorption of Cu2S thin films.

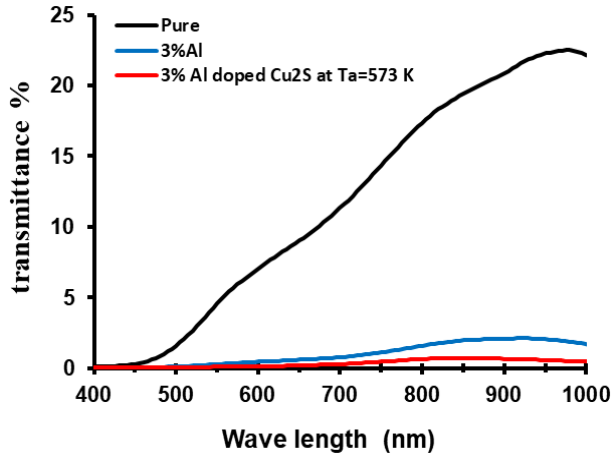

Fig. 4. Shows the permeability of Cu2S thin films as a function of wavelength.
as a function of wavelength.

Figure (6) shows plot $(\alpha\ h\nu)^2$ as a function of photon energy ($h\nu$) to calculated the visual energy gap (Eg^{opt}) values derived from Tauc's equation:[24,25]

$$(\alpha h\nu)=A(h\nu-E_g)^n \quad (3)$$

where A: is constant and n is a number that varies depending on the sort of visual transition. Cu2S thin films' visual energy gap values were showing decrease from (2.25eV) to (1.4eV) after doping and annealing which mean there is shift toward red in absorption edge, as shown in Fig. (6) and Fig. (7).This behavior can be attributed to an increase of defects as a results combination of Cu^{+2} ions by Al^{+3} ions due to the difference in ionic radii, these values get good material for solar cells.

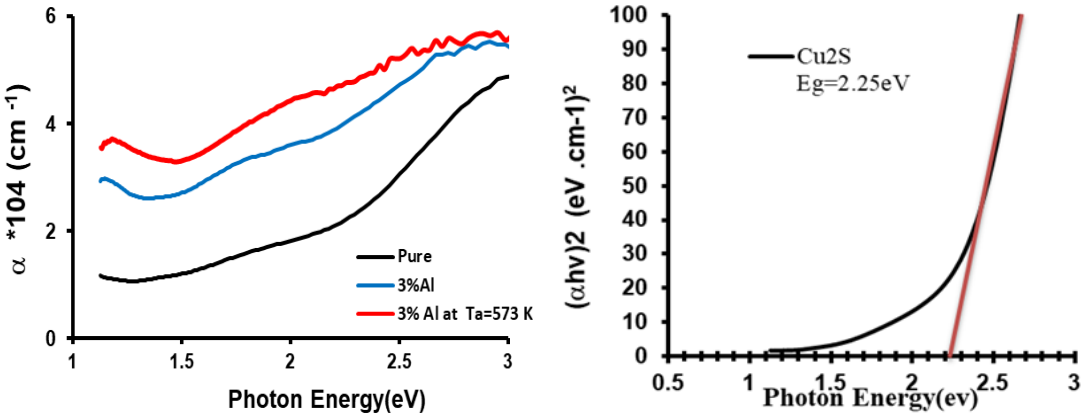

Fig. 5. Shows the relationship between the absorption coefficient and photon energy for Cu2S thin films.

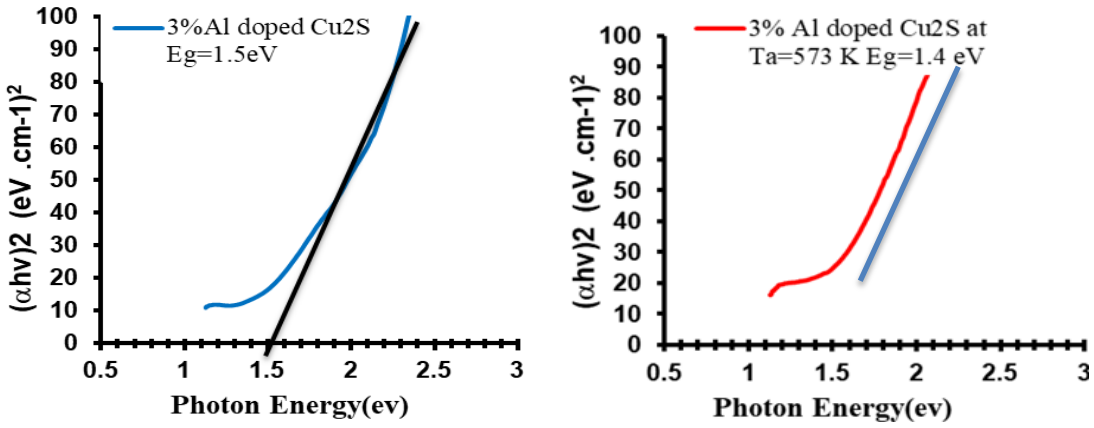

Fig. 6. Shows the relationship between $(\alpha hv)^2$ and photon energy in Cu2S thin films. a) pure at R.T b) doped 3% Al (Cu_2S:Al)at (273k) c) doped 3% Al at (Ta=573 K).

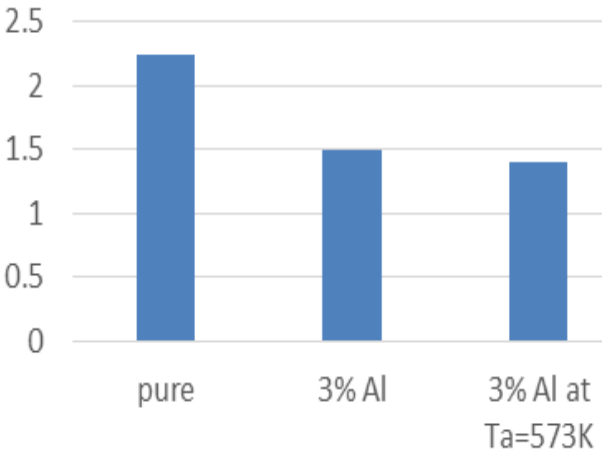

Fig. 7. Optical energy gap for Cu_2S films.

The values of refractive index can be calculated from the formula: [26]

$$n = \{[4R / (R-1)]-K^2\}^{1/2} – [(R+1) / (R-1)] \quad (4)$$

where R is the reflectance which calculated by using equation:

$$R = 1-T-A \quad (5)$$

The extinction coefficient (K) is related to absorption coefficient (α) by: [27]

$$\alpha = 4\pi K / \lambda \quad (6)$$

The refractive index (n) behavior with photon energy for (Cu_2S, Cu_2S:3%Al and Cu_2S:3%Al at Ta=573 K) films as shown in figure (8). This figure show that due to changes in the structural characteristics of films, refractive index values fall after doping and annealing at increasing photon energies.

The variation of the extinction coefficient (K) with photon energy for Cu_2S thin films pure and doped 3% Al at (R.T and Ta=573 K) is shown in Fig (9), from this figure we can notice that the extinction coefficient values increase after doping and annealing, this behavior of the extinction coefficient values similar to that of the absorption coefficients for all the range of the wavelength spectrum.

The real and imaginary part of dielectric constant (ε_1, ε_2) can be calculated from: [26]

$$\varepsilon_1 = n^2-K^2 \quad (7)$$

$$\varepsilon_2 = 2nK \quad (8)$$

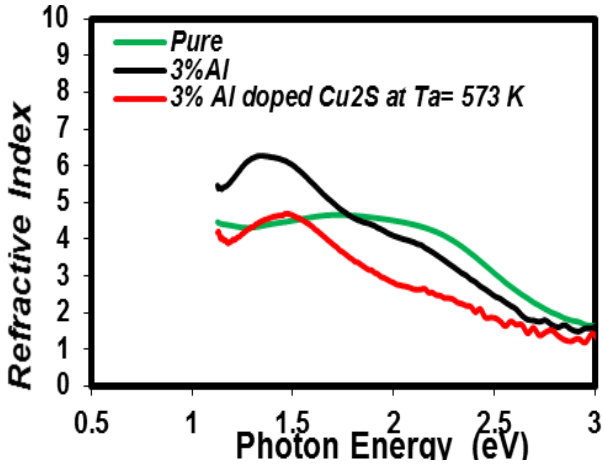

Fig. 8. Variation refractive index versus Photon energy for Cu_2S thin films.

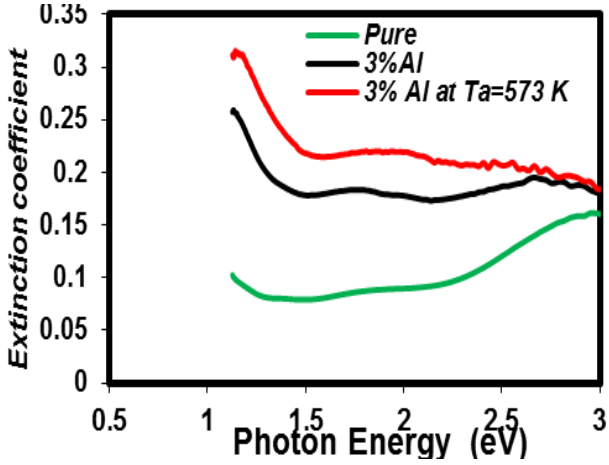

Fig. 9. Variation extinction coefficient versus Photon energy for Cu_2S thin films.

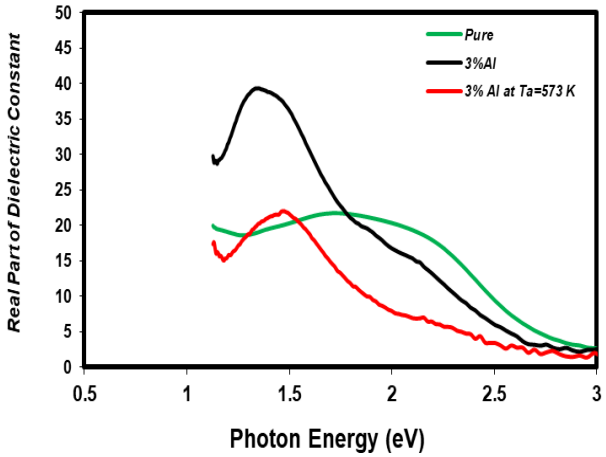

Fig. 10. Variation real part of dielectric constant Photon energy for Cu_2S thin films.

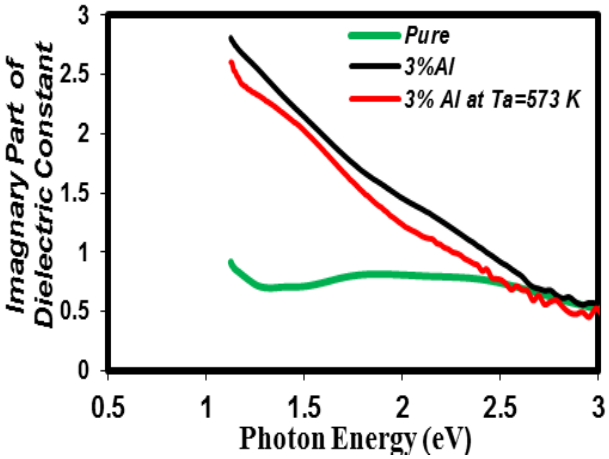

Fig. 11. Variation imaginary part of dielectric constant versus Photon energy for Cu_2S thin films.

Figures 10 and 11 shows the variation of the real (ε_1) and imaginary (ε_2) parts of the dielectric constant values versus photon energy for (Cu_2S, Cu_2S:3%Al and Cu_2S:3%Al at Ta=573 K) films. The variation of real part of the dielectric constant mainly depend on the refractive index

values while the imaginary part of the dielectric constant value mainly depend on the extinction coefficient values.

Table 3. Cu_2S thin films optical constants.

State	Eg^{opt} (eV)	Optical constant at λ = 550 nm				
		α x 10^4 cm^{-1}	n	K	ε_1	ε_2
Cu_2S	2.25	4.8	4.5	0.1	20	0.9
Cu_2S : 3% Al	1.5	5.1	6.2	0.25	40	2.8
Cu_2S : 3% Al at Ta =573k	1.4	5.9	4.8	0.3	22	2.6

3.4. Hall Measurement

Van der Pauw Ecopia-HMS -3000 was used to calculate Hall coefficient (R_H), resistivity, carrier concentrations (n_H), conductivity type and Hall mobility (μ_H) for (Cu_2S and Cu_2S:3% Al) films before and after annealing. The majority charge carriers are holes because all Cu_2S films revelation p-type conductivity. All Hall parameters are shown in Table 1.

Table 1. Hall parameter for SnS thin films.

Sample	Ta K	Average Hall coefficient R_H	Carrier concentrations n_H cm^{-3}	Mobility μ_H (cm^2/ V.S)	σ (Ω.cm)
Cu_2S	R.T	2.708×10^5	2.305×10^{13}	3.87×10^2	1.43E-3
	573	1.08×10^4	5.77×10^{14}	1.304×10^3	1.207E-1
Cu_2S:3%Al	R.T	1.15×10^{-3}	5.40×10^{21}	8.48×10^{10}	7.33E+3
	573	1.114×10^1	5.605×10^{17}	3.412×10^4	3.064E+3

It is clear from Table 1 that both (n_H) and (μ_H) for Cu_2S contrasts after doping with Al. This performance can be ascribed to the decrease charge carriers trapping centers and grain boundary scattering due to the enhanced film structure and electrical characteristic after doping.

4. Conclusion

In this search determines the influence of (3% Al) doping and annealing temperatures on structural, surface morphology, electrical and optical properties of Cu_2S thin films with thickness (400nm) deposited well by thermal evaporation method onto glass substrate. XRD results reveal the films were formed of Cu_2S phase and polycrystalline with preferential orientation in (220) direction. The crystallite size was effect after doping increased from 42 to 62 nm. The results of the AFM revealed that both grain size and surface roughness are depending on the films doping and annealing temperature. The optical energy gap decrease from 2.25 to 1.5 eV after doping. The Optical properties of these films indicating that these films are good for photovoltaic application. Hall result showed that all films have predominant p-type performance, the highest carrier concentrations and mobility was recorded for sample doped with 3% Al.

References

[1] P.Sateesh, P. Madhusudhanarao, International Journal of Advanced Research in Physical Science (IJARPS), 2(11), 11-16 (2015)

[2] R. S. Patil, T.P. Gujar, C.D. Lokhande, R.S.Mane, Sung-Hwan Han, Journal of non-crystalline Solids, 353(2007). https://doi.org/10.1016/j.jnoncrysol.2007.01.014

[3] S. Suresh, C. Raveendra Reddy, G. Suresh Babu, T. Veera Reddy, IJSDR 1(9) (2016).

[4] Nair, P. K., and Nair, M. T. S., J. PHY., D, Appl.Phy.,24, 83-88 (1991). https://doi.org/10.1088/0022-3727/24/1/016

[5] Yamamoto, T., Kubota, E., Taniguchi, A., Dev, S., Tanaka, K., and Osakada, K., Chem.Mater. 4, 570-576 (1992). https://doi.org/10.1021/cm00021a015

[6] Nair, M. T. S, and Nair, P. K., Semicond.Sci.Technol., 4,191-199. (1989). https://doi.org/10.1088/0268-1242/4/3/009

[7] Sagade, A. A., and Sharma, R., Sensors and Actuators B: Chemical 133, 135-143. (2008). https://doi.org/10.1016/j.snb.2008.02.015

[8] Pathan, H. M., Desai, J. D., and Lokhande, C. D, , Appl. Surf. Sci. 202, 47-56 (2002); https://doi.org/10.1016/S0169-4332(02)00843-7

[9] M. Ramya, and S. Ganesan, Iranian Journal of Materials Science & Engineering 8(2) (2011).

[10] P.J Sebastian, O. Gomez-Daza, J. Campos, L Banos, and P.K. Nair, Sol. Energ. Matter. Sol. C.32 159. (1994). https://doi.org/10.1016/0927-0248(94)90301-8

[11] S. Lindross, A Arnold and M Leskela, Appl. Surf. Sci. 158 75. (2000).

[12] F. Li, T. Kong, W.T.Bi, D.C.Li, and X.T. Huang, Appl. Surf. Sci. 255 6285 (2009). https://doi.org/10.1016/j.apsusc.2009.02.001

[13] J. Liu and D.F. Xue, J.cryst. Growth, 311 500 (2009). https://doi.org/10.1016/j.jcrysgro.2008.09.025

[14] Y.-J. Wang, A.-T. Tsai, C.-S. Yang, Mater. Lett., 63, 847(2009); https://doi.org/10.1016/j.matlet.2009.01.013

[15] .S.V. Bagul, S.D. Chavhan, R. Sharma, J. Phys. Chem. Solids, 68, 1623(2007); https://doi.org/10.1016/j.jpcs.2007.03.053

[16] S.G. Chen, Y.F. Huang, Y.Q. Liu, Q. Xia, H.W. Liao, C.G. Long, Mater Lett., 62, 2503(2008); https://doi.org/10.1016/j.matlet.2007.12.032

[17] . Bini, K. Bindu, M. Lakshmi, C. SudhaKartha, K.P. Vijayakumar, Y. Kashiwaba, T. Abe, Renewable Energy , 20, 405(2000); https://doi.org/10.1016/S0960-1481(99)00122-6

[18] C.G. Munce, G.K. Parker, S.A. Holt, G.A. Hope, A. Colloids Surf., 295, 152(2007); https://doi.org/10.1016/j.colsurfa.2006.08.045

[19] L. Isac, A. Duta, A. Kriza, S. Manolache, M. Nanu, Thin Solid Films, 515, 5755(2007). https://doi.org/10.1016/j.tsf.2006.12.073

[20] X. B. He, A. Polity, D. I. Osterreicher, D. Pfisterer, R. Gregor, B. K. Meyer and M. Hard, Physica B: Condensed Matter, 308, 1069(2001). https://doi.org/10.1016/S0921-4526(01)00851-1

[21] MudiXin, KunWei Li, Hao Wang, Applied Surface Science, 15, 1436(2009). https://doi.org/10.1016/j.apsusc.2009.08.104

[22] S. Schneider, J.R. Ireland, M.C. Hersam, T.J. Marks, Chem. Mater., 19, 2780(2007); https://doi.org/10.1021/cm0700495

[23] Ghuzlan Sarhan Ahmed, and Bushra K. H. Al-Maiyaly, AIP Conference Proceedings 2123, 020074 (2019).

[24] S Bushra H. Hussein, Hanan K. Hassun, NeuroQuantology 18(5), 77 (2020). https://doi.org/10.14704/nq.2020.18.5.NQ20171

[25] B. K. H. AL-Maiyal, B. H. Hussein and H. K. Hassun, Journal of Ovonic Research, 16 (5), (2020).

[26] B. K. H. AL-Maiyal , Ibn Al-Haitham J. for Pure & Appl. Sci 26(1) (2013).

[27] B. K. H. AL-Maiyal , Ibn Al-Haitham J. for Pure & Appl. Sci, 28 (3) (2015).